

# ULTRASONIC C-SCAN FOR DEFECT INSPECTION ON FLEXIBLE SOLAR MODULES

Dicky Silitonga <sup>\*1</sup>, Pooja Dubey <sup>†1</sup> and Nico F. Declercq <sup>‡1</sup>

<sup>1</sup>George W. Woodruff School of Mechanical Engineering, Georgia Institute of Technology, Atlanta, USA

## 1 Introduction

Solar photovoltaic modules are currently available in various forms and configurations. However, portable use cases often require the flexibility of the solar panels to prevent breakage easily. Defects such as breakage remain a risk even in flexible solar panels [1]. These defects may emerge as early as during the production stage. Therefore, inspection of such products is necessary in the quality control stage [2].

Ultrasonic-based inspection methods, such as C-scan and scanning acoustic microscopy (SAM), hold promising potential for detecting microscale defects in solar panels. While Ultrasonic C-scan is a mature technique widely employed across various industrial sectors, its utilization in solar modules remains uncommon. Conversely, although SAM has been applied for observing defects in solar cells [3], its efficiency in comprehensive module scanning is limited.

This paper examines the capability of C-scan in identifying microscale defects on solar panels, assessing its potential as an alternative method for defect detection in flexible solar panel manufacturing.

## 2 Method

### 2.1 Specimen

A flexible mini solar panel serves as the specimen under investigation. The specimen is a multilayered structure consisting of (from bottom to top) a PE backsheet, a metal plate, solar cells, and front transparent plastic layers. Some portions of the front plastic layers are removed to expose the solar cells, on which scratches are intentionally made.

To simulate defects, five lines of artificial scratches are introduced onto the surface at varying severity levels. The picture of the specimen with the artificial scratches, prepared for C-scan measurements, is presented in Figure 1.

### 2.2 Ultrasonic C-Scan

Scanning is conducted using a 5-axis scanning machine (IT-TransformNDT Polar C-scan), facilitating linear and angular adjustments of transducer positions. Various scanning settings are experimented, with the predetermined scanning directions and emission frequencies to generate the C-scan image. In terms of scanning directions, both scan-axes parallel and perpendicular to the scratch lines are tested.

The two modes of transducer scanning motions are illustrated in Figure 2. The scanning resolution in all measurement instances is 0.1 mm. Transducers with center frequencies of 5 MHz and 20 MHz are used in a pulse-echo setup,

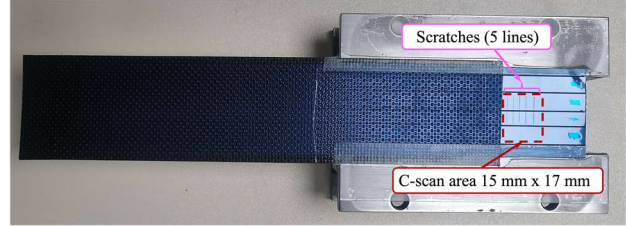


**Figure 1:** The specimen, a flexible mini solar panel, fixed on a flat mounting for c-scan experiments.

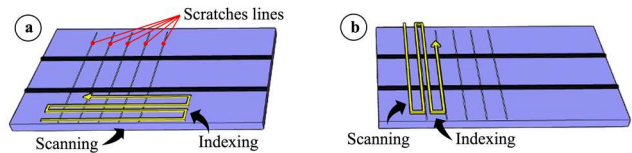


**Figure 2:** Scanning motion modes: (a) Scanning perpendicular to scratches, indexing parallel to scratches; (b) Scanning parallel to scratches, indexing perpendicular to scratches.

emitting pulses at their corresponding response spectrum, oriented at normal incidence relative to the surface.

### 2.3 Scanning Acoustic Microscopy (SAM)

To perform the microscopic imaging of the scratch, the specimen is observed under a scanning acoustic microscope (PVA-Tepla). Measurements are made with the acoustic lens of 400 MHz, scanning an area of  $800 \mu\text{m} \times 800 \mu\text{m}$  at  $2.5 \mu\text{m}$  resolution.

## 3 Results

Scanning perpendicular to the scratch lines, with indexing parallel to them, as depicted in Figure 2(a), reveals indications of the scratch lines. It is evident from the scan image in Figure 3(a). On the other hand, when scanning parallel to the scratch lines, the c-scan image does not depict the scratch lines, as demonstrated in Figure 3(b). The c-scan images represent a  $15 \text{ mm} \times 17 \text{ mm}$  area, corresponding to the region bounded within the dashed rectangle in Figure 1.

Both images in Figures 3(a) and 3(b) show results obtained from measurements conducted at 20 MHz. However, when the frequency is changed to 5 MHz, the resulting c-scan image does not indicate the presence of scratch lines. Figure 3(c) displays the image generated at 5 MHz frequency, using the scanning motion mode perpendicular to the scratch lines, which previously revealed the scratches at 20 MHz as in the Figure 3(a).

A Scanning Acoustic Microscopy (SAM) micrograph showing a segment of a scratch line is illustrated in Figure 3(d). This micrograph enables the measurement of the scratch

\* dsilitonga@gatech.edu

† pooja.dubey@gatech.edu

‡ declercq@gatech.edu

width. Utilizing the provided reference scale of 150  $\mu\text{m}$ , the scratch width measures 63  $\mu\text{m}$ .

## 4 Discussion

Results from the measurements demonstrates the variation of defects visibility, in this case the artificial scratch lines, depending on the scanning motion modes and frequency. Lower frequency, as expected, provides less sensitivity to small scale features. In this case, the feature of interest are scratch lines with the width of around 60  $\mu\text{m}$ .

However, a phenomenon worth investigating from our experiments is related to the discrepancy that arises when scanning in the different directions, see Figure 3(a) and (b), despite being performed at the same frequency of 20 MHz and at normal incidence. One possible explanation is concerning the non-symmetric beam profile of the transducer, since the beam profile has effects on the sensitivity of the measurement [4]. The position exposed to the more dominant side-lobe creates higher intensity scattering, which may happen during the measurement that produces Figure 3(a).

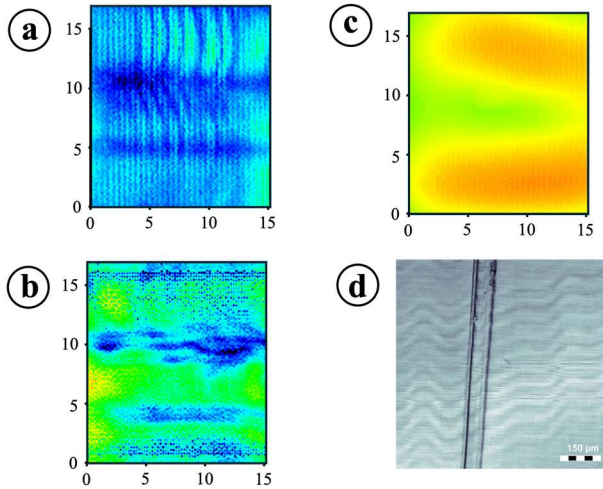


**Figure 3:** (a) 20 MHz, scan perpendicular to scratch lines; (b) 20 MHz, scan parallel to scratch lines; (c) 5 MHz, scan perpendicular to scratch lines; (d) SAM micrograph of a scratch.

Another potential factor leading to the discrepancy is because when scanning perpendicular to the crack lines, a sudden fluctuation of scattered wave occurs as the transducer momentarily passes the line, creating contrasts in the c-scan image. Meanwhile, during the scan parallel the scratch line, the scattering is relatively constant as the waves continuously interacts with the same feature along the scan path, hence producing low contrast. Further studies on the transducers' beam profile and various scanning orientations are required to verify these hypotheses.

Up to this stage, it is evident that C-scan demonstrates the capability to detect micrometer-scale defects on flexible solar panels. However, it is imperative to take into account both the direction of scanning motion and the beam profile of the transducer.

## 5 Conclusion

The present work has exhibited the capability of ultrasonic C-scan in detecting microscale defects on a flexible solar panel. While demonstrating promising potential, further investigation is necessary to enhance the performance and reliability of this method.

## References

- [1] L. Papargyri *et al.* Modelling and experimental investigations of microcracks in crystalline silicon photovoltaics: A review. *Renew. Energy*, 145, 2020.
- [2] M. Aghaei *et al.* Review of degradation and failure phenomena in photovoltaic modules. *Renew. Sustain. Energy Rev.*, 159, 2022.
- [3] A. Belyaev, O. Polupan, S. Ostapenko, D. Hess, and J. P. Kalejs. Resonance ultrasonic vibration diagnostics of elastic stress in full-size silicon wafers. *Semicond. Sci. Technol.*, 21, 2006.
- [4] J. Shi, S. Liu, F. Liu, and G. Xun. Multi-mode ultrasonic visualization of porosity in composites using a focused transducer with high sensitivity and near-surface resolution. *Compos. Part C Open Access*, 4, 2021.